Supplementary Material

Supplementary material to the different sections in Fischereit J., Larsén X. G., Hahmann A. N. (2022) *Climatic impacts of wind-wave-wake interactions in offshore wind farms*.

1 SUPPLEMENTARY MATERIAL TO THE METHODS

1.1 Selection of representative days

Table S1 shows the applied filter criteria to quality control the different measurements before applying them to selection of representative days.

Table S1. Filtering criteria applied to the different variables. U is wind speed, D is wind direction, H_s is significant wave height, θ_p and θ_m are peak and mean wave direction.

Variable	Criterion	Reference
U	Gross range test: $[0, 75]\,\mathrm{ms}^{-1}$ Spike test: $< 10\,\mathrm{ms}^{-1}$	Word Meteorological Organization (2007)
D	Gross range test: $[0, 360]\,^\circ$	Word Meteorological Organization (2007)
U & D	$U = 0$ & $D = 0$; $U \neq 0$ & $D \neq 0$	Word Meteorological Organization (2007)
H_s	Gross range test: $[0.001, 16]$ m; 0.001 m is used instead of 0.01 because of buoys in tidal areas Station-specific gross range test: $3\,\mathrm{m} \leq \begin{cases} (\max - P_{99.99}) & P_{99.99} < 8\,\mathrm{m} \\ (P_{99.9} - P_{99}) & \text{else} \end{cases}$	Coastal Data Information Program (2021)
θ_p, θ_m	Gross range test: $[0, 360]\,^\circ$	Coastal Data Information Program (2021)

Figure S1 shows the monthly availability of samples after filtering the base sample stations to include only times with at least 22 hour availability at two consecutive days. It also shows the monthly distribution of sampled days in the selected sample.

Figure S2 shows as an example for one resample set for the 10-m wind speed the climatic PDF Z^c and sample PDFs $Z^s_{N(t)}$ for different N with the same collection of dates t at one of the base sample stations, here Heligoland in the North Sea, along with the corresponding Perkins Skill Score PSS. As the sample size increases, the PSS increases, indicating a better fit of the climatic PDF.

Figure S3a to Figure S6a show ERA5 30-year averages for different parameters along with the average over the 180 selected sample days at different stations. Figure S3b to Figure S6b show boxplots of the measurement climate and ERA5 climate per station as well as the respective boxplots for the 180 sample days.

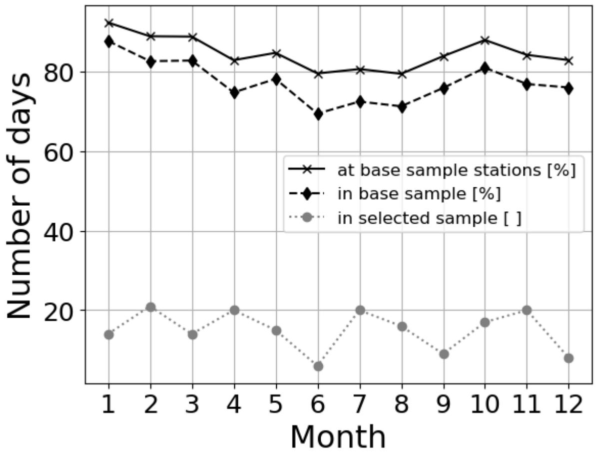

Figure S1. Monthly distribution different sample matrices within the 30-year period.

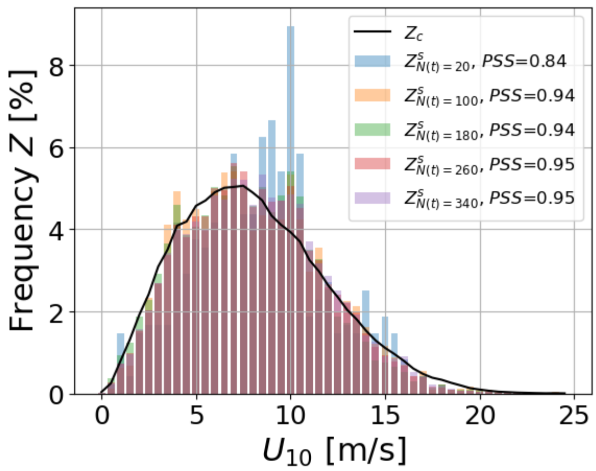

Figure S2. Example frequency distributions for wind speed at 10 m height (U_{10}) at Heligoland for the climate Z^c and for the frequency distribution $Z^s_{N(t)}$ of randomly sampled pairs of two consecutive days of different sizes N with the corresponding PSS.

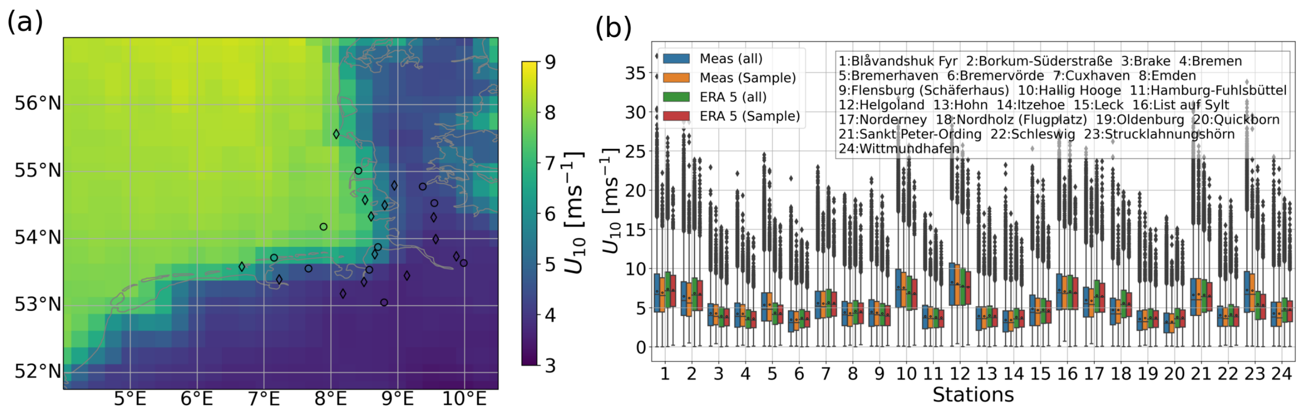

Figure S3. ERA5 30-year average (a) wind speed in 10 m height (U_{10}) with diamonds showing the reprensentativity of the 180 selected days. (b) U_{10} boxplots of measurement climate (blue) and ERA5 climate (green) per station as well the respective boxplot from the 180 sample days.

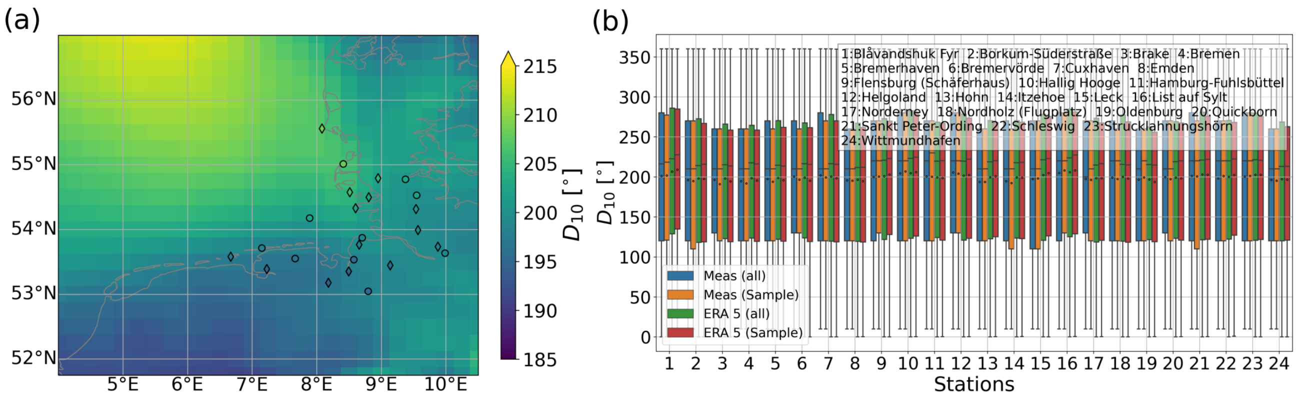

Figure S4. As Figure S3 but for wind direction in 10 m height (D_{10}).

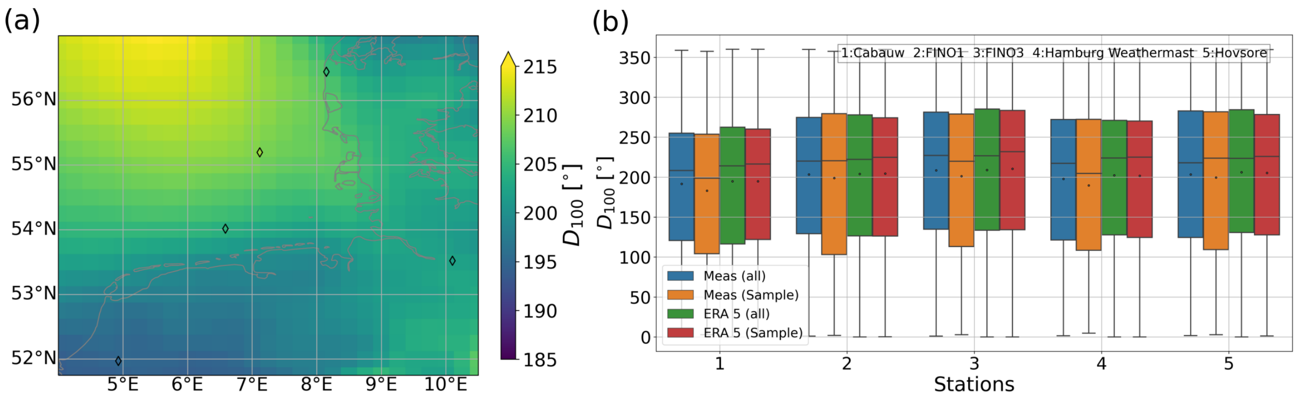

Figure S5. As Figure S3 but for wind direction in 100 m height (D_{100}).

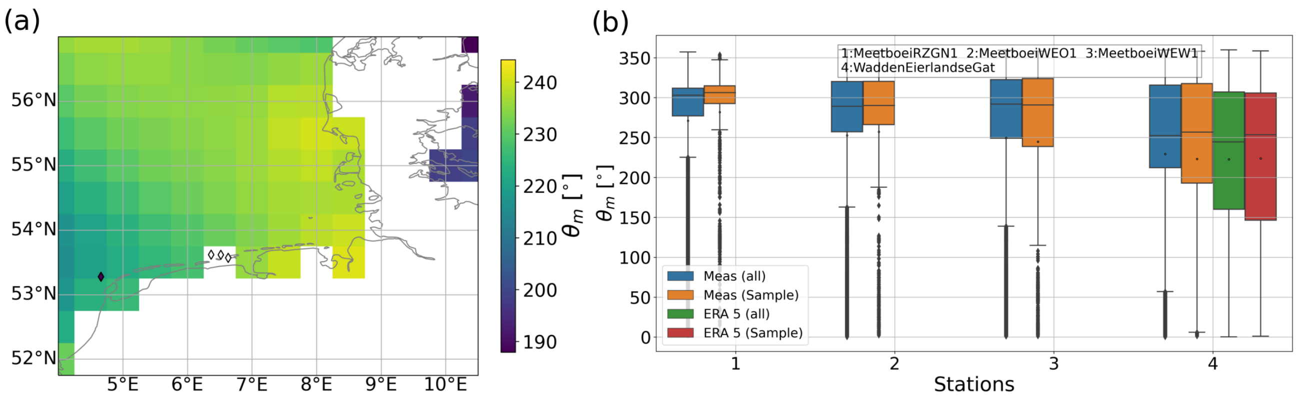

Figure S6. As Figure S3 but for mean wave direction (θ_m).

1.2 Modeling system and set-up

Table S2 shows the details for the model set-up of WRF and SWAN.

Table S3 summarizes the applied wind turbine characteristics for the different simulated wind farms.

Table S2. Set-up of WRF and SWAN.

Category	Model	Subcategory	Details (WRF option number)
Time	Simulation length		2.5 days, 12 h spin-up
	Output time step		10 min
	WRF	time step	45 s
	SWAN	time step	6 min
	Coupling	exchange time step	6 min
Resolution	WRF, SWAN	horizontally	18 km, 6 km, 2 km with one-way nesting
	WRF	vertically	62 sigma levels up to a model top of 50 hPa with 24 (mass) levels in the lowest 250 m, i.e. about 10 m spacing in the lowest levels
	SWAN	frequency	61 frequencies between 0.03 Hz and 10.05 Hz with a frequency exponent of 1.1
		direction	36 bins
Boundary and forcing data	WRF	dynamical forcing	ER5
		land use data	CORINE
		sea surface temperature	OSTIA
		land surface model	NOAH-LSM (2)
	SWAN	bathymetry	1/8 arc-minute bathymetry data from EMODnet Digital Terrain Model (DTM)
		Boundaries	Open boundaries of outer domain set to zero
		initial conditions	Spectra of a previous uncoupled 24-hour-long SWAN simulation
Schemes	WRF	PBL	MYNN (5)
		Surface layer	MO (2)
		Microphysics	WRF Single-Moment (WSM) 5-class scheme (4)
		Radiation	RRTMG scheme (4)
		Cumulus parameterisation	Kain-Fritsch scheme (1) only in domain 1
		Diffusion	Simple diffusion (1) 2D deformation (4) 6th order positive definite numerical diffusion (2) rates of 0.06, 0.08 and 0.1 for domain 1, domain 2 and domain 3 vertical damping.
		Advection	Positive definite advection of moisture and scalars (1), activated TKE advection
	WFP	EWP	$r_{0,frac}$=1.7
		FIT	TKE factor 0.25
	SWAN	Wave breaking	Constant, $\alpha = 1.0$ and $\gamma = 0.73$
		Bottom friction	JONSWAP $cf_{jon} = 0.038$
		Wind input and whitecapping	WBLM

Table S3. Wind farm details for all simulated wind farms. Note that for some wind farms the applied turbine model does not correspond to the actually installed one, since thrust and power curves for that particular model was not available. Nevertheless, the chosen hub-height and rotor-diameter correspond the actual installed one. Turbines marked with [1] are scaled from NREL 5 MW turbine and turbines marked with [2] are scaled from DTU 10 MW turbine. For the Haliade150-6MW turbine the thrust and power curves for SWT-6.0-154 are used. Power curves for SWT-7.0-154 is scaled from SWT-6.0-154, while keeping the thrust curve. Similarly, 6.3M152 is scaled from 6.2M126, but with adjusted dimensions.

Wind farm	Turbines	Turbine Model	Hub Height [m]	Rotor top [m]	Wind Farm Area [km^2]
Albatros	16	SWT-7.0-154	105.0	182.0	11
Alpha Ventus	12	M5000-116[1], Senvion_5M[1]	90.0, 92.0	148.0, 155.0	4
Amrumbank West	80	SWT-3.6-120	88.0	148.0	30
BARD Offshore	80	M5000-116[1]	90.0	148.0	59
Borkum Riffgrund 1	78	SWT-4.0-120	89.5	149.5	36
Borkum Riffgrund 2	56	VestasV164-8.0	105.0	187.0	36
Butendiek	80	SWT-3.6-120	88.0	148.0	31
Deutsche Bucht	31	VestasV164-8.0	105.0	187.0	18
Gemini	150	SWT-4.0-130	95.0	160.0	68
Global Tech I	80	M5000-116[1]	90.0	148.0	40
Gode Wind 1	55	SWT-6.0-154_110	110.0	187.0	40
Gode Wind 2	42	SWT-6.0-154_110	110.0	187.0	29
Hohe See	71	SWT-7.0-154	105.0	182.0	40
Horns Rev I	80	V80-2.0	67.0	107.0	21
Horns Rev II	91	SWT-2.3-93	68.3	114.8	33
Horns Rev III	49	VestasV164-8.0	105.0	187.0	144
Meerwind Süd/Ost	80	SWT-3.6-120	88.0	148.0	40
Merkur Offshore	66	Haliade150-6MW	103.0	178.5	39
Nordsee One	54	6.2M126_90[2]	90.0	153.0	30
OWP Nordergründe	18	6.2M126_84[2]	84.0	147.0	3
OWP Nordsee Ost	48	6.2M126_95[2]	95.0	158.0	36
OWP Veja Mate	67	SWT-6.0-154	106.0	183.0	51
Offshore Windfarm DanTysk	80	SWT-3.6-120	88.0	148.0	65
Offshore Windfarm Sandbank	72	SWT-4.0-130	95.0	160.0	47
Offshore Windpark Riffgat	30	SWT-3.6-120	88.0	148.0	6
Trianel Windpark Borkum	40	M5000-116[1]	90.0	148.0	23
Trianel Windpark Borkum II	32	6.3M152	104.5	180.5	23

2 SUPPLEMENTARY MATERIAL TO THE RESULTS

2.1 Evaluation of the modelling system performance

Figure S7 shows a density scatter plot of the drag coefficient (C_D) derived from simulated surface roughness length (z_0) against simulated 10-m wind speed (U_{10}) for WRF+SWAN for (a) FINO1 and (b) FINO3 for all simulated days. The mean and standard deviation for different U_{10} classes are shown as solid and dotted orange lines, respectively. Empirical relationships derived from measurement campaigns are shown as lines and have been reproduced from Larsén et al. (2019).

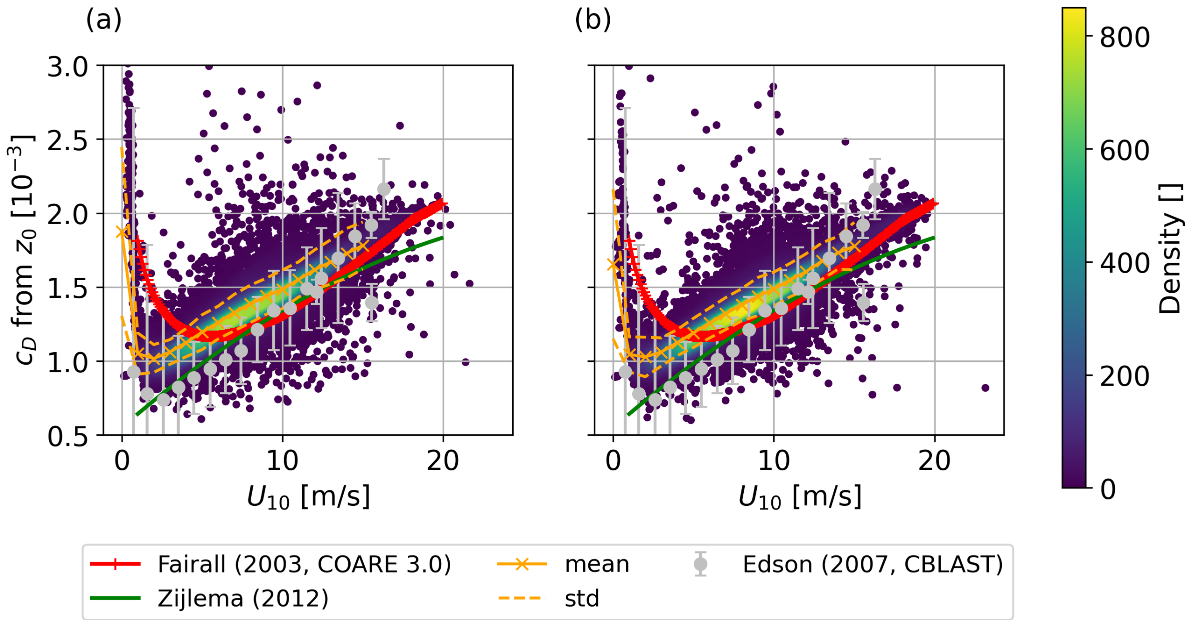

Figure S7. Density scatter plot of drag coefficient (C_D) derived from simulated surface roughness length (z_0) against simulated 10-m wind speed (U_{10}) for WRF+SWAN for (a) FINO1 and (b) FINO3 for all simulated days. Mean and standard deviations over from the simulations are shown as orange lines. Other lines show empirical relationships derived from measurement campaigns.

2.2 Impacts on hub-height wind

2.2.1 Impacts of wind farms

Figure S8 shows the simulation results and relative differences between scenarios for 10-m Turbulent Kinetic Energy (TKE_{10}). The involved scenarios for the subtraction are in the titles of each sub-figure and all relative differences are normalized with the subtrahend.

Figure S9 shows the simulation results and standard deviations of the difference between scenarios for 100-m wind speed (U_{100}). The involved scenarios for the subtraction are in the titles of each sub-figure.

Figure S10 shows exemplary (a,d,g,j) the simulated 100-m wind speed distribution for WRF and WRF+FIT for 4 sites as shown in (c,f,i,l) along with (b,e,h,k) difference distribution for (WRF+FIT)-WRF. The p-value (p) in (b,e,h,k) is derived from the performed t-test for which the results are spatially shown in Figure S11 as dotted hatched area for $p < 0.01$.

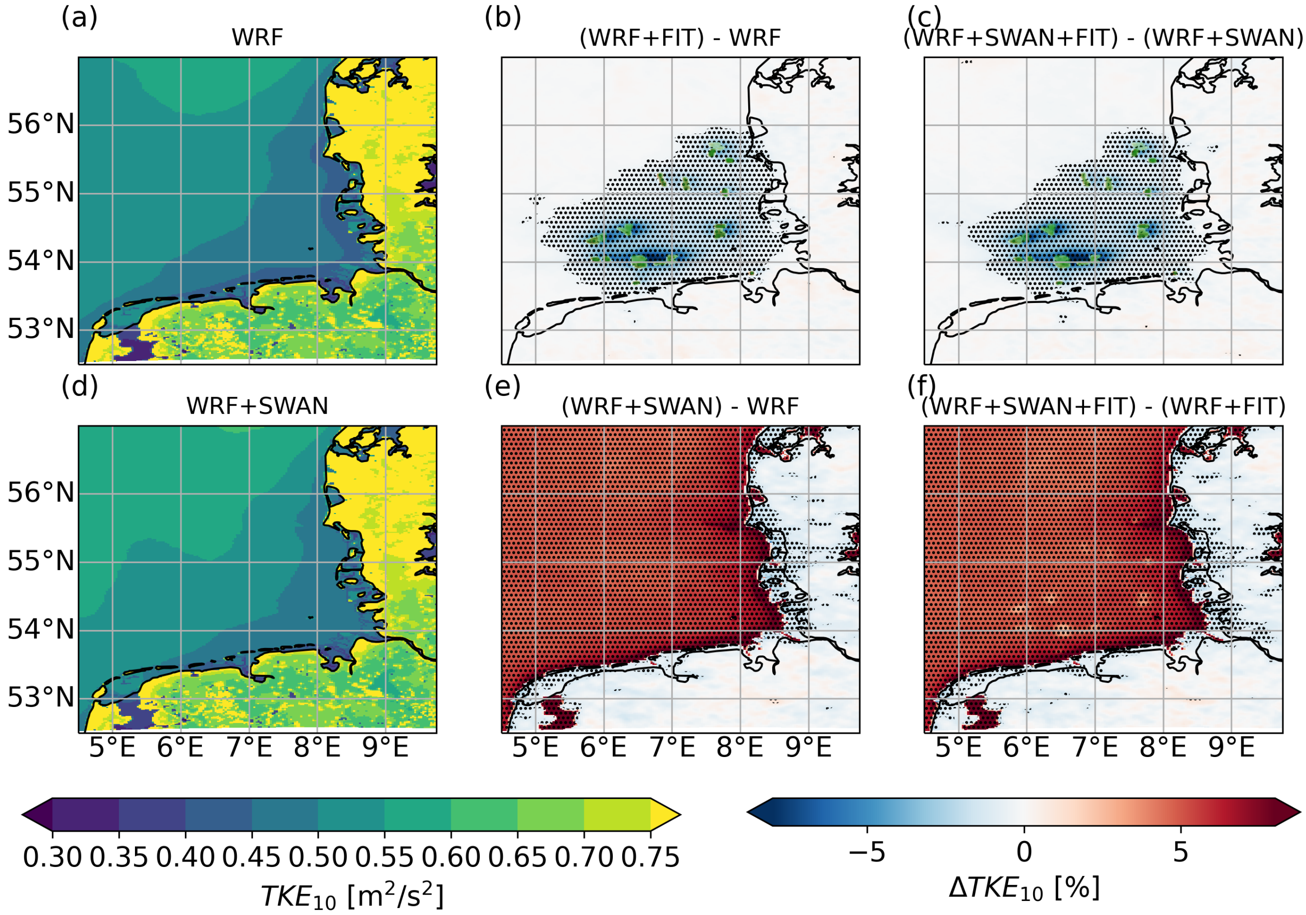

Figure S8. (a,d) Turbulent Kinetic Energy at 10 m height (TKE_{10}) for stand-alone WRF and coupled WRF+SWAN simulations as well as (b,c) relative differences between a simulation with Fitch wind farm parameterization and a simulation without wind farms and (e,f) relative differences between a coupled simulation and an uncoupled simulations. Dotted hatched area in (b,c,e,f) show significant differences and wind farms in (b,c) are shown in green.

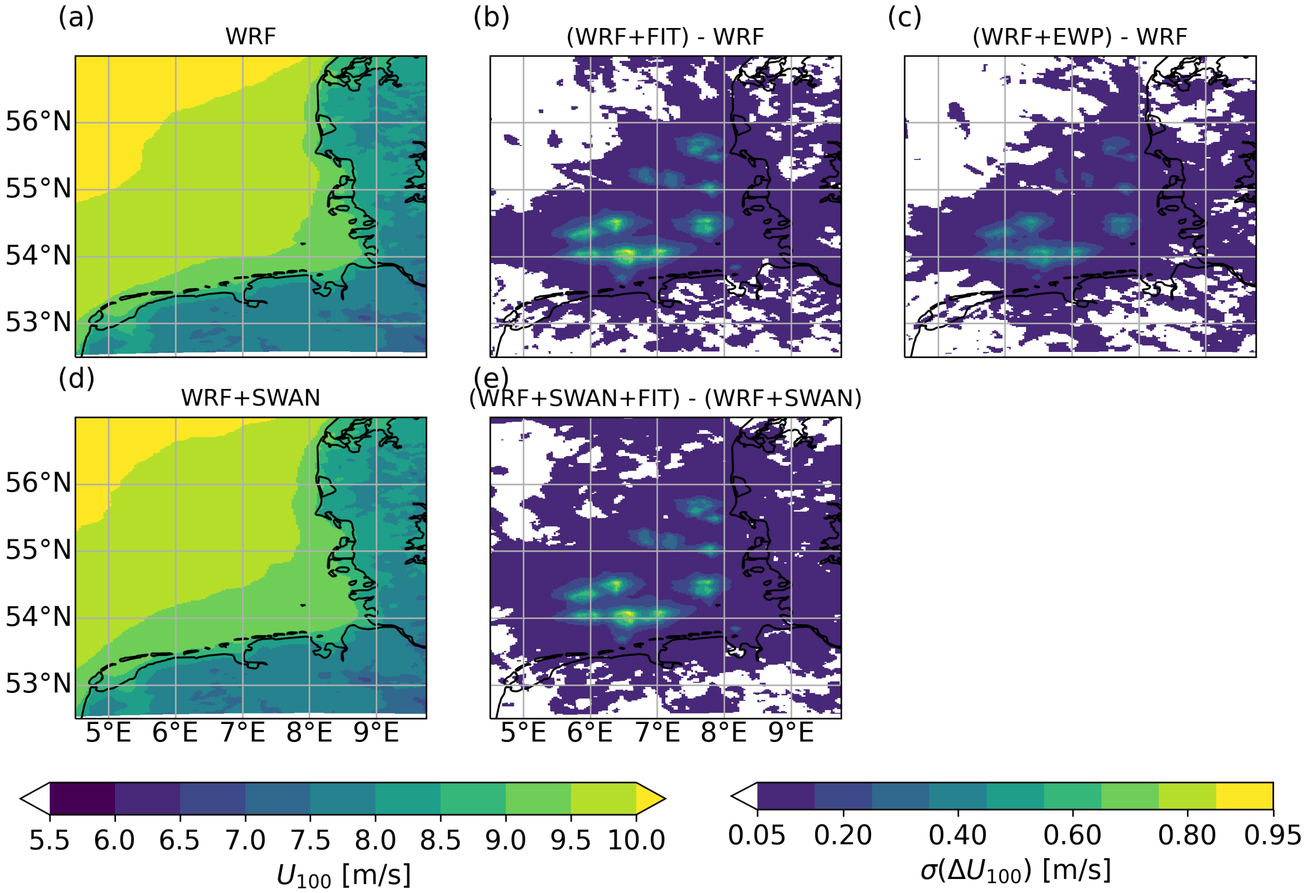

Figure S9. (a,d) Simulated wind climate at 100 m height for (a) WRF and (d) WRF+SWAN and (b,c,e) standard deviation of the difference of wind speed based on (b) (WRF+FIT)-WRF, (c) (WRF+EWP)-WRF and (e) (WRF+SWAN+FIT)-(WRF+SWAN).

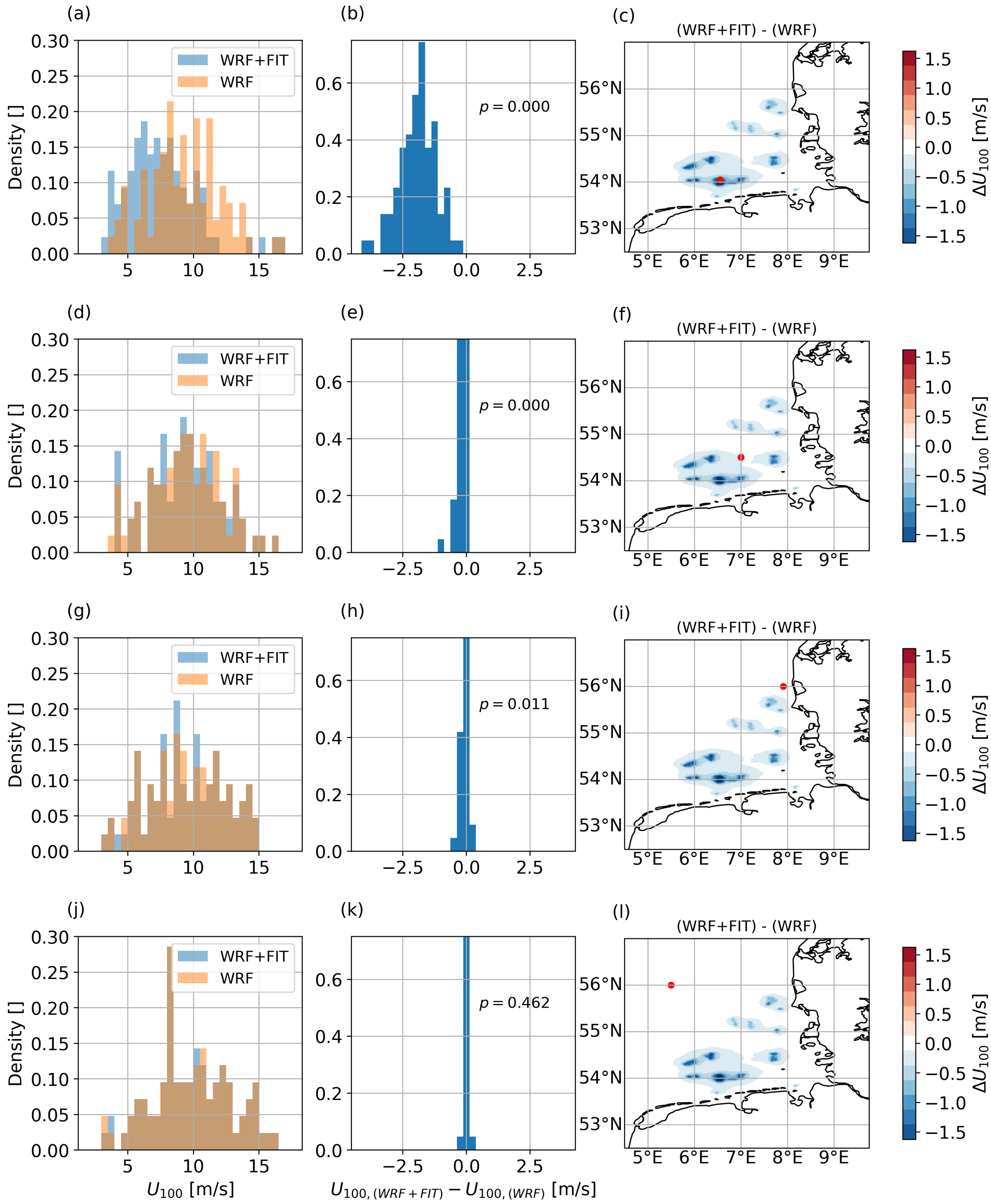

Figure S10. (a,d,g,j) histogram of wind speed at 100 m height for (blue) WRF+FIT and (orange) WRF, (b,e,h,k) histogram of the difference of (WRF+FIT)-WRF and (c,f,i,l) the locations (red dot) for each row. The p-value (p) in (b,e,h,k) refers to the t-test in Figure S11.

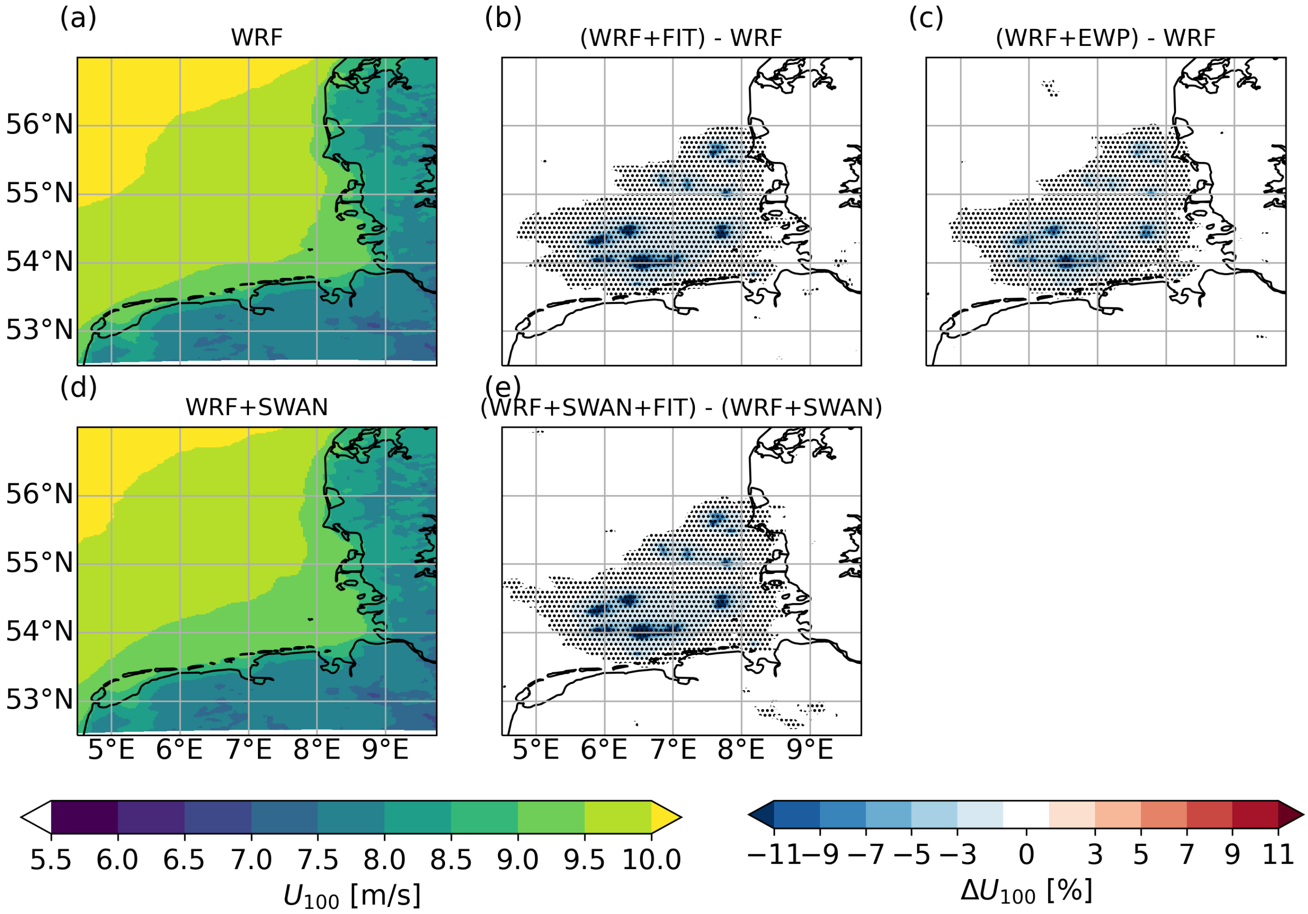

Figure S11. Same as Figure S9, but for (b,c,e) the relative reduction of wind speed based on (b) (WRF+FIT)-WRF, (c) (WRF+EWP)-WRF and (e) (WRF+SWAN+FIT)-(WRF+SWAN). The dotted hatched area indicates significant difference (see main text).

2.2.2 Impacts of waves

Similarly as Figure S9 and Figure S11, Figure S12 and Figure S13 show the for the difference between coupled and uncoupled simulation, the standard deviation and the area of significant differences for the wind climate at 100 m height.

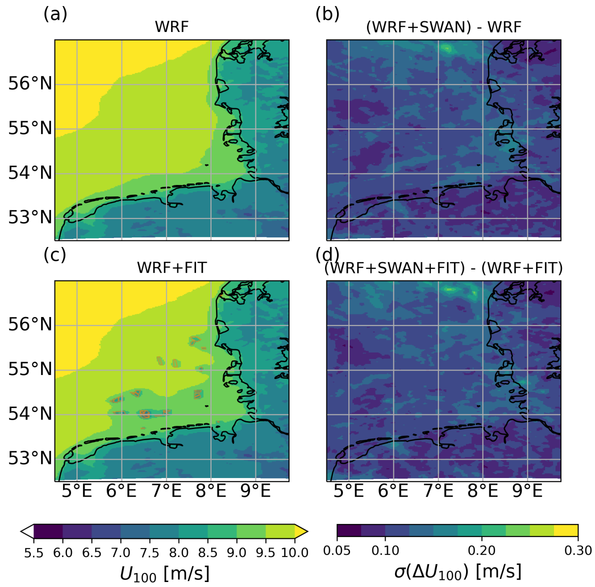

Figure S12. (a,c) Simulated wind climate at 100 m height for (a) WRF and (c) WRF+FIT and (b,d) standard deviation of the difference of wind speed based on (b) (WRF+SWAN)-WRF, (d) (WRF+SWAN+FIT)-(WRF+FIT).

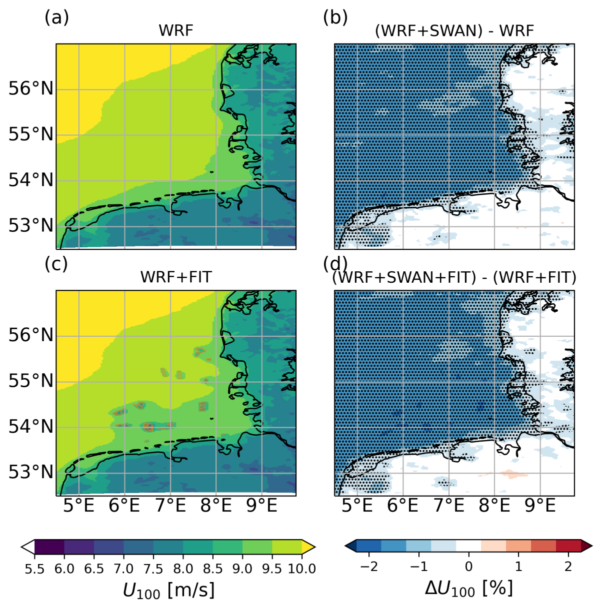

Figure S13. Same as Figure S12, but for (c,d) the relative reduction of wind speed based on (b) (WRF+SWAN)-WRF, (d) (WRF+SWAN+FIT)-(WRF+FIT). The dotted hatched area indicates significant difference (see main text).

Figure S14 shows profiles of (a) wind speed and (b) absolute and (c) relative wind speed difference between coupled and uncoupled simulations with wind farms as average over the center point of all wind farms (ochre dots in (d,e)), dense wind farms (purple diamonds in (d,e)) or no wind farms (red crosses in (d,e)).

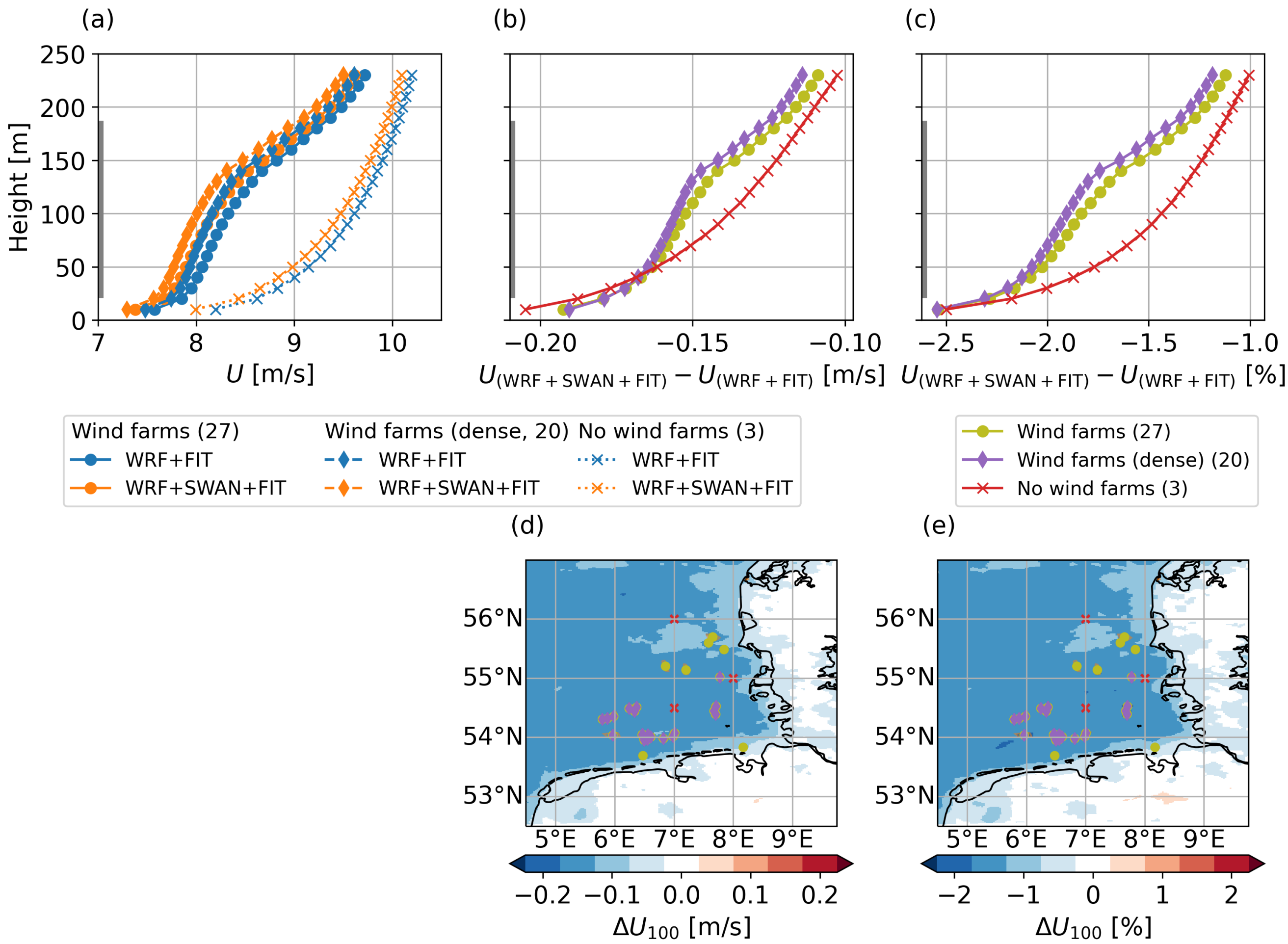

Figure S14. Temporal mean profiles of (a) wind speed and (b) absolute difference in wind speed between WRF+SWAN+FIT and WRF+FIT and (c) relative difference in wind speed between WRF+SWAN+FIT and WRF+FIT normalized with WRF+FIT for 3 areas consisting of averages over several grid points: center of wind farms (27 grid points, ochre dots in (d,e)), dense wind farms (20 grid points, purple diamonds in (d,e)) and no wind farms (3 grid points, red crosses in (d,e). Map of differences at 100 m height for (d) absolute differences and (e) relative differences.

Figure S15 shows the difference of $\Delta U_{100} = U_{100,WRF+SWAN+FIT} - U_{100,WRF+FIT}$ of the mean over the center points of all wind farms and the mean over 3 sites outside the farms together with the slope of the mean thrust coefficient over all farms. ΔU_{100} outside the farms is subtracted to better isolate the effect of the wind farm alone.

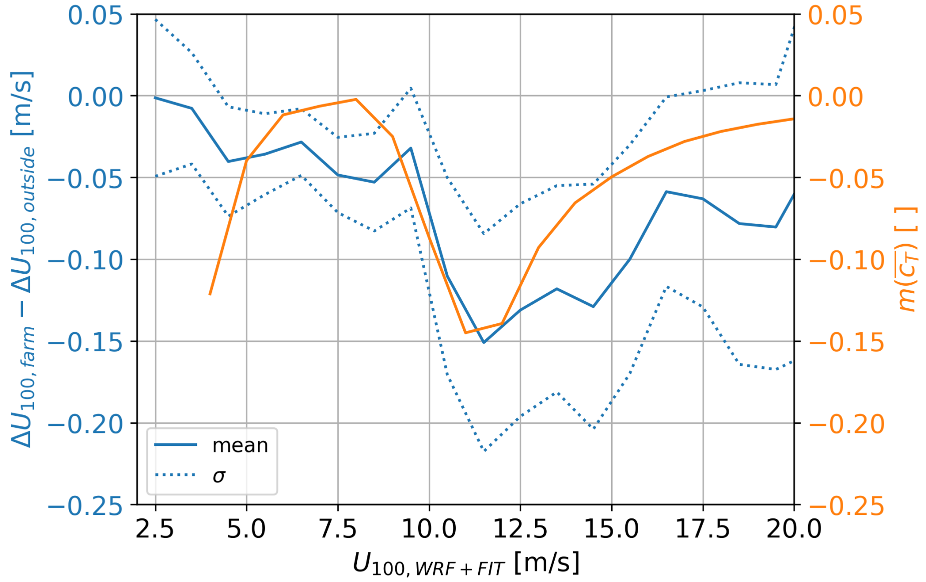

Figure S15. For different wind speed classes at 100 m for WRF+FIT the (left axis) difference of $\Delta U_{100} = U_{100,WRF+SWAN+FIT} - U_{100,WRF+FIT}$ as average over center points of all wind farms (ochre dots in Figure S14) and over 3 sites outside wind farms (red crosses in Figure S14) and (right axis) slope of the average thrust curves of all turbines.

2.3 Impacts on waves

Figure S16 is the same as Figure S8 but for 10-m wind speed (U_{10}). Figure S17 and Figure S18 are the same as Figure S9 and Figure S11 but for significant wave height (H_s).

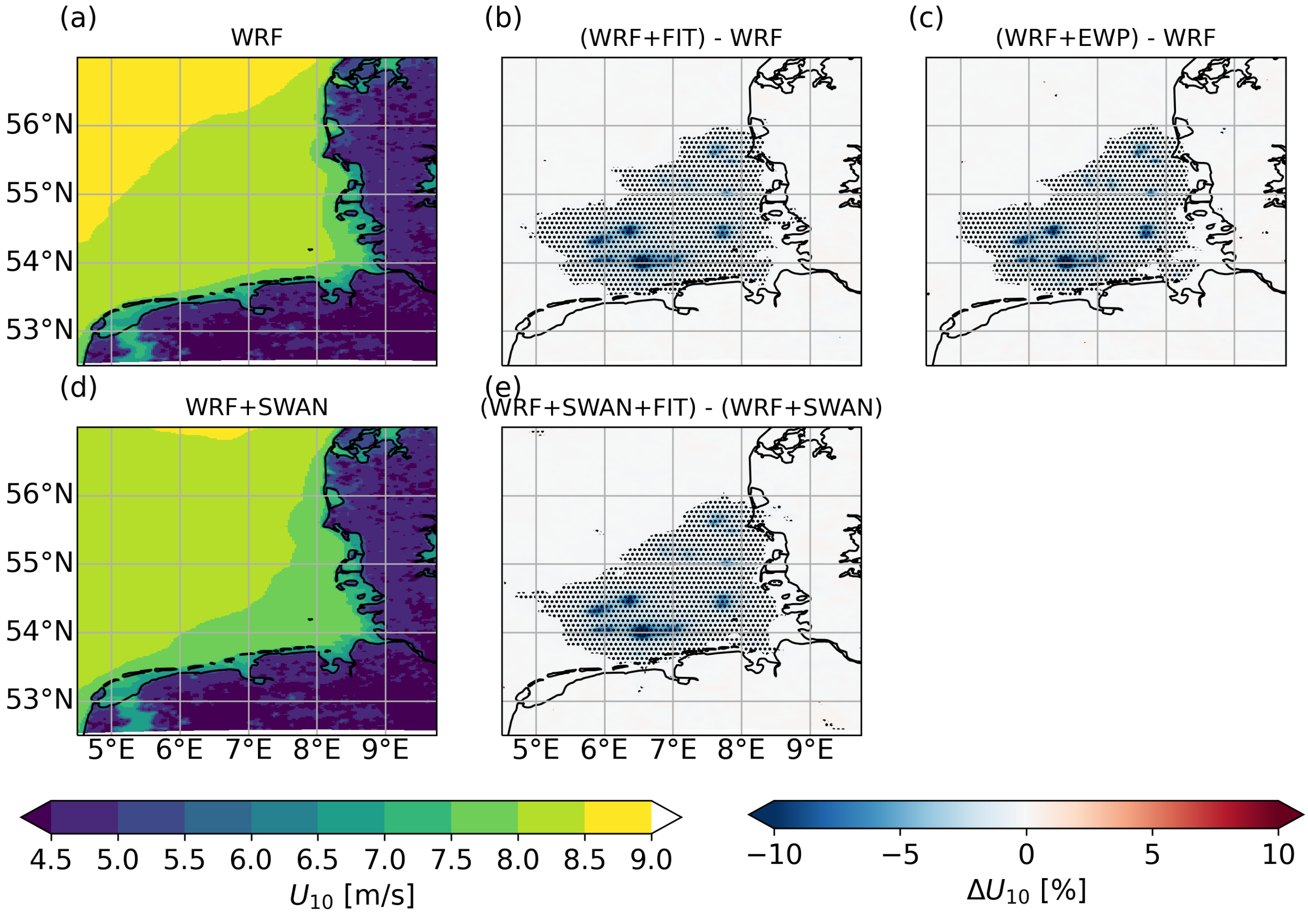

Figure S16. (a,b,d,e) same as Figure S8a,b,c,d but for wind speed in 10 m height (U_{10}) and (c) relative differences between a simulation with EWP wind farm parameterization and a simulation without wind farms.

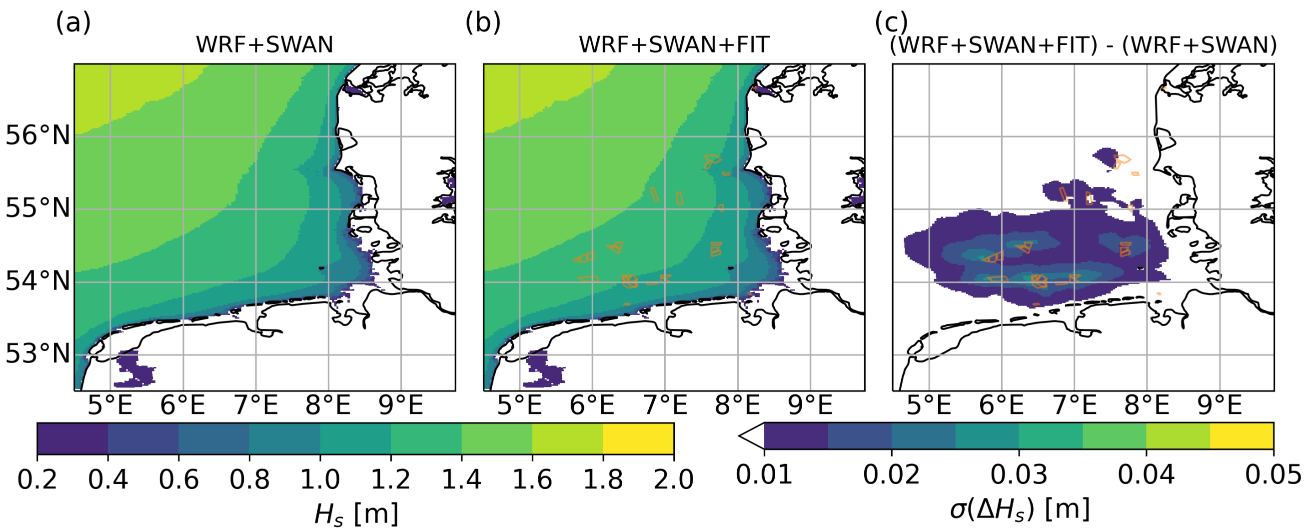

Figure S17. (a,c) Simulated climate of significant height for (a) WRF+SWAN and (b) WRF+SWAN+FIT and (c) standard deviation of the difference of significant wave height based on (WRF+SWAN+FIT)-(WRF+SWAN).

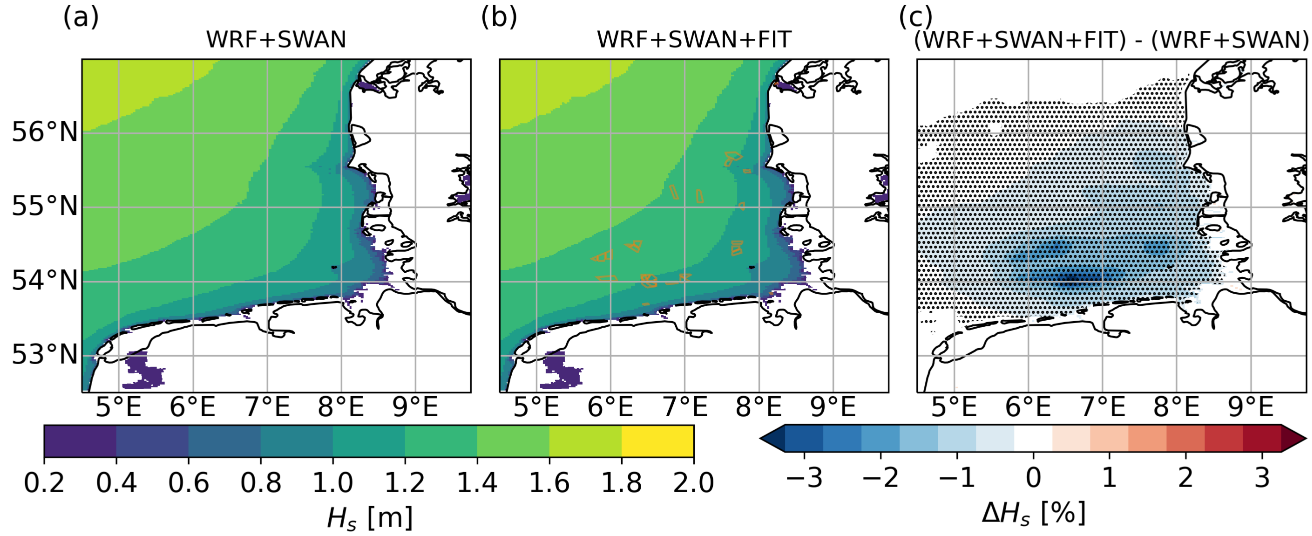

Figure S18. Same as Figure S17, but (c) for the relative reduction of significant wave height based on (WRF+SWAN+FIT)-(WRF+SWAN). Dotted hatched area in (c) indicates significant differences.

3 SUPPLEMENTARY MATERIAL TO THE DISCUSSIONS AND CONCLUSIONS

Figure S19 shows the long-term average for (a) inverse wave age U_{10}/c_p, where c_p is the wave velocity at the peak frequency and (b) the angle between wind direction at 10 m height and peak wave direction. Both are based on WRF+SWAN simulations as averages over all simulated days.

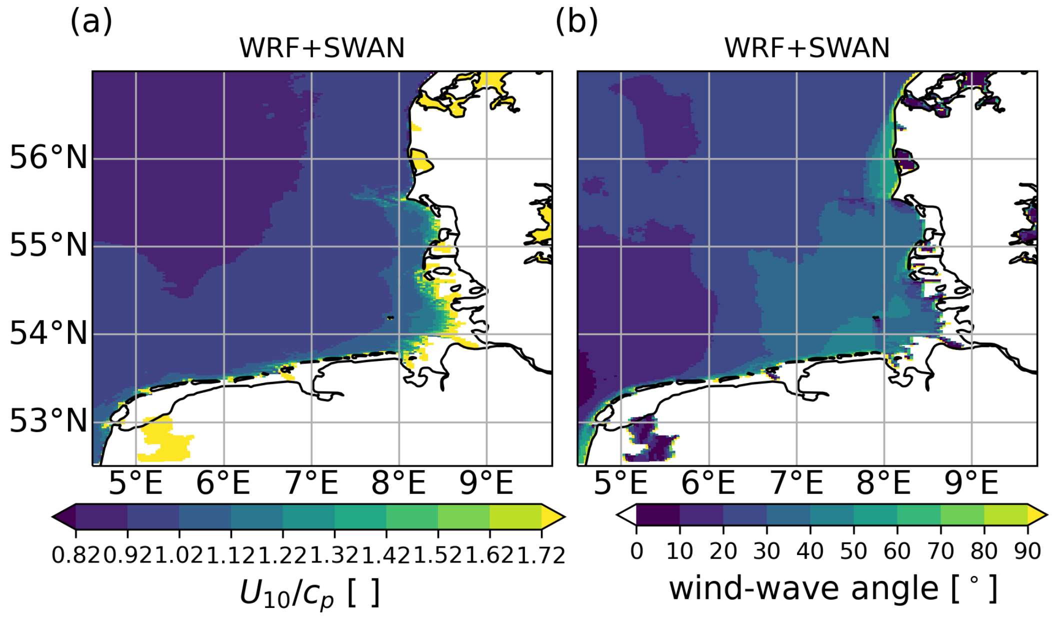

Figure S19. Climatic averages of (a) inverse wave age and (b) wind-wave misalignment from WRF+SWAN simulations.

REFERENCES

[Dataset] Coastal Data Information Program (2021). Data Processing — CDIP 1.1 documentation

Larsén, X. G., Du, J., Bolaños, R., Imberger, M., Kelly, M. C., Badger, M., et al. (2019). Estimation of offshore extreme wind from wind-wave coupled modeling. *Wind Energy* 22, 1043–1057. doi:10.1002/we.2339

Word Meteorological Organization (2007). *Guide to the Global Observing System*. Tech. rep., Word Meteorological Organization, Geneva WMO-No. 488, third edition